Mon. Not. R. Astron. Soc. **000**, 000–000 (0000) Printed 26 June 2009 (MN LATEX style file v2.2)

Differential stellar population models: how to reliably measure [Fe/H] and [α/Fe] in galaxies

C.J. Walcher[1]⋆, P. Coelho[2], A. Gallazzi[3], and S. Charlot[2]
[1]*Research and Scientific Support Department, European Space Agency, Keplerlaan 1, 2200AG Noordwijk, The Netherlands*
[2]*Institut d'Astrophysique de Paris, CNRS, Université Pierre & Marie Curie, UMR 7095, 98bis, bd Arago, 75014 Paris, France*
[3]*Max Planck Institut für Astronomie, Königstuhl 17, 69117 Heidelberg, Germany*

ABSTRACT

We present differential stellar population models, which allow improved determinations of the ages, iron and α-element abundances of old stellar populations from spectral fitting. These new models are calibrated at solar abundances using the predictions from classical, semi-empirical stellar population models. We then use the predictive power of fully synthetic models to compute predictions for different [Fe/H] and [α/Fe]. We show that these new differential models provide remarkably accurate fits to the integrated optical spectra of the bulge globular clusters NGC6528 and NGC6553, and that the inferred [Fe/H] and [α/Fe] agree with values derived elsewhere from stellar photometry and spectroscopy. The analysis of a small sample of SDSS early-type galaxies further confirms that our α-enhanced models provide a better fit to the spectra of massive ellipticals than the solar-scaled ones. Our approach opens new opportunities for precision measurements of abundance ratios in galaxies.

Key words: methods: data analysis, globular clusters: general, galaxies: abundances, galaxies: elliptical

1 INTRODUCTION

Stellar population models designed to understand the photospheric emission from stars in galaxies and star clusters have reached an impressive degree of maturity in the last decade (e.g. Vazdekis 1999; Bruzual & Charlot 2003; Le Borgne et al. 2004; Vázquez & Leitherer 2005).

A remaining problem is that theoretical stellar spectra are not mature enough to reproduce real stars at all spectral types and complete wavelength range in an absolute sense (e.g. Martins & Coelho 2007; Bertone et al. 2008). The most common solution is to replace in the optical wavelength regime the theoretical stellar spectra with spectra derived from empirical spectral libraries. We call such models "semi-empirical". A draw-back of these models has always been that the stellar spectra are restricted to the abundance patterns present in the empirical libraries (dominated by solar neighbourhood stars). So, while semi-empirical models provide an excellent basis for solar metallicity and [α/Fe]=0 (e.g. Asari et al. 2007; Koleva et al. 2008), they are biased at non-solar metallicites.

To overcome these biases, we here use the predictive power of the fully theoretical models from Coelho et al. (2007, hereafter C07) to compute *relative* changes in flux F_λ as a function of [Fe/H] and [α/Fe]. These are then applied to the solar abundance SSPs from semi-empirical models, yielding "differential population synthesis models" that are at the same time highly accurate in an absolute sense and whose predictions for non-solar abundance patterns are well-defined and unbiased. The new differential models are accurate enough to reliably determine the (over-)abundance of the α-elements from the integrated spectrum of an old stellar population. Predicting and fitting every pixel in the spectrum, as compared to predicting the Lick indices "only" (Trager et al. 2000; Thomas et al. 2004), allows one to (1) use the redundancy of the information at different wavelengths, for data of lower S/N, (2) analyse spectra at higher resolution (3) explore wavelength ranges not covered by Lick indices and (4) free oneself of potentially complicated corrections for instrumental and velocity dispersion.

2 COMPUTING DIFFERENTIAL MODELS

Semi-empirical stellar population models provide a reliable zero-point for the spectral evolution of stellar populations of solar metallicity (more precisely [Fe/H]=0 and [α/Fe]=0, called "solar" for the remainder of this letter). We therefore rely on them for the absolute calibration (including their stellar evolutionary tracks). For the present letter, we used Bruzual & Charlot (2003, hereafter BC03), Le Borgne et al. (2003, hereafter PegHR), and an updated version of Vazdekis (1999, hereafter V09) and we refer to these papers for a complete description.

For the pixel-by-pixel corrections (subsequently called "differentials") as a function of [Fe/H] and [α/Fe] we rely on the purely theoretical models computed by C07 and we refer to this paper for

⋆ E-mail:jwalcher@rssd.esa.int

all details. The models predict the spectra of SSPs in the age range 3 to 14 Gyr, in the wavelength range 3000 Å to 1.34 μm, and for the abundance values [Fe/H] = −0.5, 0.0 and 0.2 and [α/Fe] = 0.0 and 0.4 at a constant resolution of full width at half-maximum (FWHM) = 1 Å. We additionally interpolated the models for [Fe/H] = −0.25 and [α/Fe] = 0.2 in order to obtain a finer grid. The interpolation is done linearly in log(Flux). This is because the absorption caused by a single line of an element species is proportional to the exponentiated opacity, while the opacity itself depends linearly on element abundance. We will refer to this grid of 120 SSPs as the C07 models. We make the usual assumption that the fully theoretical models correctly predict the flux variation as a function of varying [Fe/H] and [α/Fe] (e.g. Trager et al. 2000; Thomas et al. 2004).

The differential recalibration procedure involves the following steps: (1) The SSP spectrum by C07 is convolved with a gaussian filter and then resampled to achieve the same resolution and binning as the semi-empirical SSP spectra used for calibration. (2) At a given age, the differential at each pixel as a function of [Fe/H] and at fixed [α/Fe]=0 is defined as the flux ratio of the SSP flux of a given [Fe/H] to the spectrum with [Fe/H] = 0.0. (3) Similarly, the ratios between the α-enhanced fluxes and solar-scaled fluxes, at the same [Fe/H], give the differential as a function of [α/Fe]. (4) All semi-empirical models were interpolated in log(Flux) to provide the same SSP ages as C07. (5) The last step is then to multiply the solar SSP fluxes of the semi-empirical models by the correction vectors derived from the fully theoretical models.

As a result we obtain three sets of differential models (one for each calibrator) at the same grid points in age, [Fe/H] and [α/Fe] as the C07 models. We will refer to these as BC03+C07, PegHR+C07, and V09+C07, respectively.

For illustration we show one of the derived differentials, namely for [Fe/H]=−0.5 and [α/Fe]=0.0 (Z=0.005), in Figure 1. It is clear that the main signal of the variation in [Fe/H] is constrained to specific wavelength ranges, such as e.g. the MgB feature. For comparison with previous work we also show the differentials of the semi-empirical models in Figure 1. We interpolated the semi-empirical models in log(Flux) to fall on [Fe/H]=−0.5[1].

The differentials derived from the semi-empirical SSPs are significantly bluer than their theoretical counterparts. Insight into this problem can be gained by overplotting in Figure 1 the differential of the C07 model for the same total metallicity (Z=0.005) but with [α/Fe]=0.4 and therefore [Fe/H]=−0.85 (obtained by extrapolation in log(Flux)). This new differential shows the same effect as the semi-empirical models, only even stronger. Indeed, the stars with sub-solar [Fe/H] represented in the stellar libraries are generally α-enhanced due to the correlation between [Fe/H] and [α/Fe] that is inherent to the solar neighbourhood (see e.g. Figure 8 from Bensby et al. 2005). Semi-empirical models thus are biased to [α/Fe]>0 at subsolar metallicities. The new differential models are free of this bias and even predict the change of the SSP spectra with [α/Fe].

We emphasize that the above differential procedure accounts for the effects of abundance variations both on stellar evolution and on stellar spectra. It is therefore more accurate than methods based on the correction of only stellar spectra (Prugniel et al. 2007; Cervantes et al. 2007). We note that the difference in the stellar evolution prescriptions of the C07 and the semi-empirical models should have only a minor influence on the differentials, as illustrated by the similarity of the results obtained for semi-empirical models with 3 different prescriptions in Figure 1.

[1] The models are generally defined in total metallicity Z and not in [Fe/H]; under the assumption of solar abundance ratios, i.e. [α/Fe]=0, [Fe/H]=−0.5 is equivalent to Z=0.005.

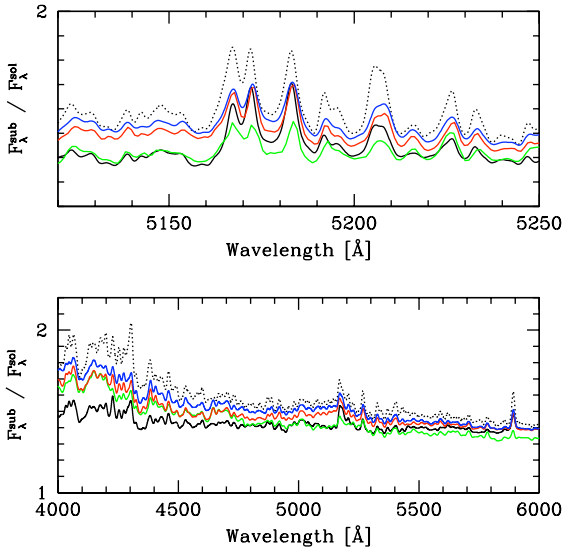

Figure 1. The ratios between SSPs of 10Gyr at subsolar metallicity (Z=0.005, [Fe/H]=−0.5, [α/Fe]=0) and solar metallicity ([Fe/H]=0,[α/Fe]=0)) for different stellar population models (black C07, green BC03, blue PegHR and red V09). The dotted line is C07 at the same Z=0.005, but different abundance ratios ([Fe/H]=−0.85 and [α/Fe]=0.4). All models have been smoothed to a common resolution of σ=1Å in the upper panel and σ=5Å in the lower panel.

3 PIXEL-FITTING OF SPECTRA

In order to test the applicability of the model spectra on observational data, we use a pixel-fitting software previously used and fully described in Walcher et al. (2006), hereafter `sedfit`. In brief, the software uses an initial template to obtain a reasonable value for the velocity and velocity dispersion of the object through a χ^2-biased random walk. Then, a non-negative least squares algorithm (Lawson & Hanson 1974) performs the inversion onto the stellar population model. Finally, the χ^2-biased random walk is repeated to yield a best estimate for the kinematic parameters.

Like the many other pixel-fitting softwares in existence (e.g. Tojeiro et al. 2007; Ocvirk et al. 2006; Cid Fernandes et al. 2005; Koleva et al. 2008), this approach has the advantage of being able to fit the kinematics and composite stellar populations simultaneously. It also provides for a convenient way to mask spectral regions either in the observed frame (CCD defects, sky lines) and/or in the rest-frame (emission lines, regions badly fit by the models).

We caution that the fit results are sensitive to the continuum normalization method. Continuum-normalized spectral fitting has been favoured by e.g. Wolf et al. (2007) over other methods as the most reliable to simultaneously retrieve age and metallicity from the integrated spectra of stellar clusters. After extensive testing, we settled for a simple running mean with exclusion of 3σ outliers as the most robust procedure. The wavelength window over which the mean was evaluated was set to cover 90 Å (compare Koleva et al. 2008).

Table 1. Properties of GCs from colour-magnitude diagrams and high-resolution stellar spectroscopy

Name	Age[Gyr]	[Fe/H]	[α/Fe]
NGC6528	11±2[1]	−0.10 ± 0.2[2]	+0.1±0.1[2]
NGC6553	11±2[3]	−0.20 ± 0.1[4]	+0.25 ±0.1[3]

[1] Feltzing & Johnson (2002); [2] Zoccali et al. (2004); [3] Alves-Brito et al. (2006); Meléndez et al. (2003)

4 APPLICATION TO GLOBULAR CLUSTERS

We now test the newly prepared differential models on high quality globular cluster spectra of NGC6528 and NGC6553 taken from Schiavon et al. (2005) [2]. Only these two bulge GCs have [Fe/H] in the range probed by the differential models. For NGC6528 six spectra are available for consistency checks. Table 1 lists the published ages and abundances of these clusters. Not all literature measurements have assigned errorbars and we have been forced to assign hopefully realistic ones ad hoc.

We fit the spectra of the GCs using the three different differential model sets (BC03+C07, V09+C07, PegHR+C07). While an extensive test of the C07 models is beyond the scope of this Letter, we also quote the results obtained with these models alone to illustrate the improvement provided by the differential models. The best-fitting SSP is determined by simply computing χ^2 for every SSP with the three different parameters age, [Fe/H], [α/Fe]. The only purpose of using `sedfit` in this context is to automatically adapt for small shifts in velocity and for the resolution of the data.

An example fit is shown in Figure 2. Over the limited wavelength range of this fit, the model looks remarkable. A more quantitative measure is the reduced χ^2, which is between 2 (for NGC6528_b_1 with PegHR+C07) and 10 (for NGC6528_a_1 with BC03+C07). While thus the fit is not perfect, we note that an SSP with solar abundance ratios yields a reduced χ^2 that is between 10% and 50% worse. Combining the realism of semi-empirical models and the predictive power of purely theoretical ones into the differential models thus leads to a significant improvement in the fit.

We repeat the fits for different ranges in wavelength. From the outset, we exclude the wavelength region below 4000 Å, as there are still not fully explained problems with semi-empirical models in this range (e.g. Wild et al. 2007; Walcher et al. 2008). We also exclude the region above 5800 Å, which has some dubious features in the data.

The wavelength regions we tested are, in order of increasing coverage:
R1: 5142-5364 Å (MgB and Fe5335 indices)
R2: 4828-5364 Å (main Lick index range)
R3: 4828-5600 Å (red extension)
R4: 4500-5600 Å (blue extension)
R5: 4000-5800 Å (full wavelength range)

In Figure 3 we show the dependence of the quartet reduced χ^2, age, [Fe/H], and [α/Fe] on the adopted wavelength range and for the spectrum NGC6528_a_2. Based on all plots for the 7 different GC spectra that we used, we find that for wavelength region R2 (4828 to 5364 Å) the parameters [Fe/H] and [α/Fe] of the best-fit SSP are in good agreement with the literature values for all differential models and all observed GC spectra. On the other hand,

[2] The spectra can be downloaded from http://www.noao.edu/ggclib/description.html.

[tbp]

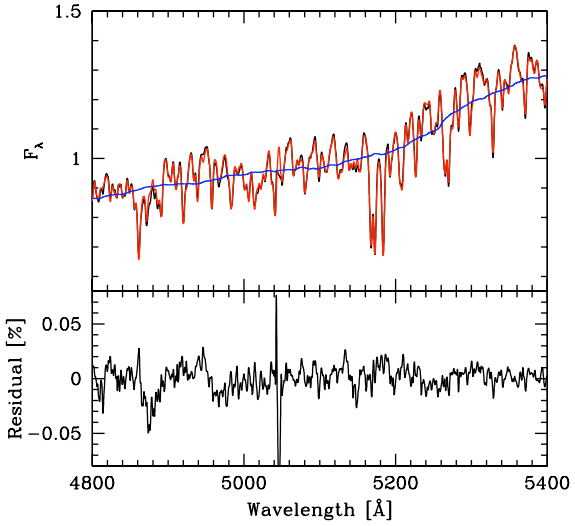

Figure 2. The spectrum of NGC6528 (black), labelled a_2, as taken from Schiavon et al. (2005) and the best-fitting model from PegHR+C07 (red). The blue line is the continuum that was used to normalize the observed spectrum. The model was fit to the data only in the wavelength range 4828-5364 Å.

the results for the other wavelength ranges scatter more and seem in particular affected by the age-[Fe/H] degeneracy. In the case of R1, the available signal may not be strong enough. In the cases of large wavelength ranges, we expect that all models become less reliable, so small uncertainties in the modelling might dominate the fit results. Concerning age, we confirm the results of Koleva et al. (2008) that the spectral fitting ages for these clusters tend to be younger than the CMD ages. This is potentially attributable to contamination by blue bulge stars or blue straggler stars in the aperture covered by the integrated GC spectra and visible in the CMD (G. Beccari, priv. comm.) or to dispersion in the Helium abundances (Catelan et al. 2009), but we note also that the CMD ages do differ by a few Gyrs in the literature.

It seems to be of rather little relevance, which semi-empirical model one uses, as inside the regions in wavelength and parameter space that we test here, the differential models behave similarly. We nevertheless note that the PegHR+C07 model yields the lowest overall χ^2 but also systematically lower ages (and higher [Fe/H]), while fitting with the BC03+C07 models seems to be most stable with respect to wavelength range between 4500-5600 Å. As expected, the fully theoretical models show a larger χ^2 and the derived values tend to be less stable than those of the differential models.

In Figure 4 we show the distribution of χ^2 as a dependence of the three parameters age, [Fe/H], and [α/Fe] for the NGC6553 spectrum. The known age-[Fe/H] degeneracy is clearly visible. There is also a slight degeneracy between [Fe/H] and [α/Fe], following a line of constant total metallicity.

5 TEST ON SDSS EARLY-TYPE GALAXIES

We now fit the spectra of a small sample of early-type galaxies from the SDSS survey (Abazajian & Sloan Digital Sky Survey 2008). Early-type galaxies are known to be enhanced in α-elements

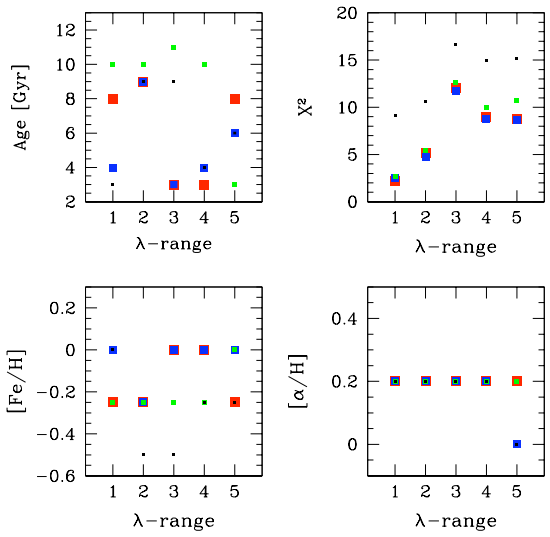

Figure 3. The dependence of the best fit parameters on the wavelength range that was used for the fit and on the model. The numbers of the wavelength ranges are given in the text of Section 4. We show results for one spectrum (NGC6528_a_2) and for all models, i.e. V09+C07 (red), PegHR+C07 (bue), BC03+C07 (green), C07 (black).

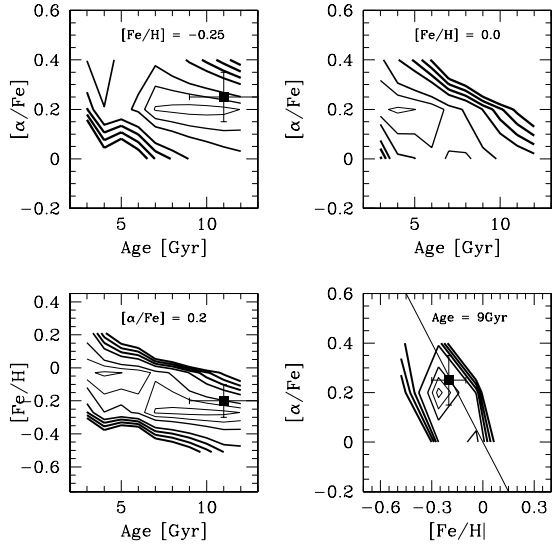

Figure 4. The distribution of χ^2 for the NGC6553_a_1 spectrum and determined over the wavelength region 4828-5364 Å, depending on the SSP parameters age, [Fe/H], and [α/Fe] using the V09+C07 model. The thicker the line the higher the value of χ^2, in steps of $\Delta\chi^2 = 1$. The squares with errorbars show the literature values from Table 1. The upper right panel shows that it is important to obtain both [Fe/H] and [α/Fe] correctly, in order to avoid a biased age measurement. In the lower right panel the locus of constant total metallicity Z=0.017 is indicated by a thin straight line.

(Worthey et al. 1992; Trager et al. 2000; Vazdekis et al. 2001; Thomas et al. 2004) and we expect this to be reflected in the best fit results. We select a subsample of 150 galaxies from the SDSS sample of Gallazzi et al. (2006). The objects have been chosen in three bins of stellar mass, log($M_*/M_\odot$) = [10-10.3], [10.7-11], [11.3-11.6]. In each mass bin we include only the first 50 galaxies with the highest S/N and with Δ(MgB/<Fe>) within 0.1 of the typical value for the mass range according to the linear fit in Gallazzi et al. (2006) (Δ(MgB/<Fe>) is an empirical estimate of [α/Fe]).

In order to test the validity of the differential models on the SDSS early-type spectra we use `sedfit` to fit the star formation history of the galaxies in a non-parametric way with two sets of templates ranging in age from 3 to 12 Gyr: once with the templates [Fe/H] = -0.25 and [α/Fe] = 0 and once with [Fe/H] = -0.25 and [α/Fe] = 0.2. The fit was carried out using the V09+C07 model in the wavelength range 4828 to 5364 Å.

Figure 5 shows that, while low-mass early-types are equally well fitted by scaled-solar than by alpha-enhanced models, for more massive early-types [α/Fe]=0.2 models provide on average a better fit. This reflects the expected mass-dependence of α-enhancement in local early-type galaxies. We hold this result to show that the differential models represent the spectra of early-type galaxies in the SDSS in a realistic way, over the whole spectrum between 4828 and 5364 Å.

The choice of values for [Fe/H] and [α/Fe] in Figure 5 is motivated by the distribution of the sample in these parameters as measured using the differential models. Nevertheless, due to the degeneracy between [Fe/H] and [α/Fe] noted in Figure 4, similarly good fits are obtained when increasing [Fe/H] to 0.0, but the best fit [α/Fe] would be shifted down by roughly 0.1 in compensation. A more thorough discussion of the impact of this degeneracy, a comparison with the global metallicities derived by Gallazzi et al. (2006) and the implications of the results for the [Fe/H] and [α/Fe] distribution of SDSS early-type galaxies will be presented in a forthcoming paper (Gallazzi et al., in prep.).

6 SUMMARY

We have computed new, differential stellar population models. These combine (1) the realism of semi-empirical models at solar metallicities, due to the recently collected extensive libraries of stellar spectra, and (2) the predictive power of purely theoretical models, due to recent advances in the computation of purely theoretical stellar spectra (Percival et al. 2009; Coelho et al. 2007).

We fitted the models to high-quality, public spectra of two globular clusters in the range of parameters covered by the new models. We showed that our best fit age, [Fe/H] and [α/Fe] are in excellent agreement with those determined by other methods in the literature. Finally we fitted a sample of 150 early-type galaxies from the SDSS and show that the reduced χ^2 is better for a model with [α/Fe] = 0.2 than for one with [α/Fe] = 0.0 for galaxies more massive than $\sim 10^{10.5}$M$\odot$, again in accordance with independent measurements from indices.

The reduced χ^2 values of the models on SDSS spectra are close to 1. We caution that this is not yet true for the highest S/N data of galactic globular clusters. Nevertheless, the uncertainties in the modelling are now *smaller* than the effects of the varying abundances over a significant wavelength range (4828 to 5364 Å). It needs to be pointed out though, that metallicity estimations from fitting the full optical spectrum, as done e.g. in Panter et al. (2008) and MacArthur et al. (2009), are still rather uncertain. On the other hand, spectral fitting allows to use the redundant information on a large part of the spectrum and to adapt automatically for changing velocity dispersions, thus it yields tight constraints even for a large sample of intermediate S/N spectra such as those of the SDSS.

We conclude that the differential models can reproduce accurately the detailed spectra of galaxies, thus allowing to measure [Fe/H] and [α/Fe] in galaxies on an absolute scale and with high

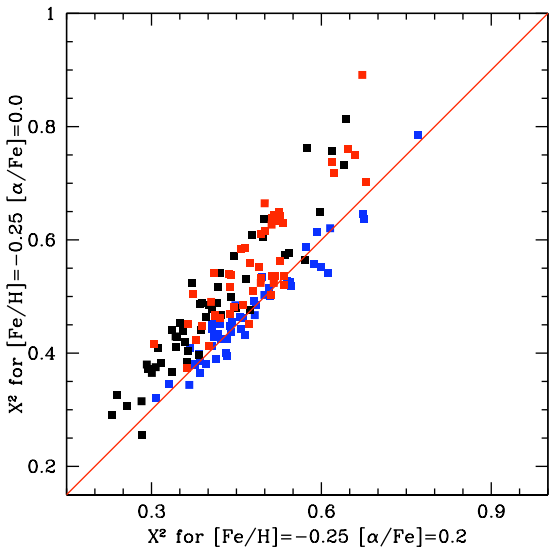

Figure 5. The reduced χ^2 of a composite age fit to the spectra of a sample of 150 early-type galaxies from the SDSS at fixed [Fe/H]=-0.25 and [α/Fe]=0.2 (abscissa) and [α/Fe]=0.0 (ordinate). Objects are split by mass, with the lowest in blue, intermediate in black and high-mass objects in red.

accuracy. With future improvements in semi-empirical and in theoretical models, differential stellar population models will become even more powerful.

ACKNOWLEDGMENTS

We thank the referee for valuable comments that led to an improved presentation of the results in this letter. P. Coelho is supported by a European Marie Curie incoming fellowship.

Funding for the SDSS and SDSS-II has been provided by the Alfred P. Sloan Foundation, the Participating Institutions, the National Science Foundation, the U.S. Department of Energy, the National Aeronautics and Space Administration, the Japanese Monbukagakusho, the Max Planck Society, and the Higher Education Funding Council for England. The SDSS Web Site is http://www.sdss.org/. The SDSS is managed by the Astrophysical Research Consortium for the Participating Institutions.

REFERENCES

Abazajian K., Sloan Digital Sky Survey f. t., 2008, ArXiv e-prints
Alves-Brito A., Barbuy B., Zoccali M., Minniti D., Ortolani S., Hill V., Renzini A., Pasquini L., Bica E., Rich R. M., Meléndez J., Momany Y., 2006, A&A, 460, 269
Asari N. V., Cid Fernandes R., Stasińska G., Torres-Papaqui J. P., Mateus A., Sodré L., Schoenell W., Gomes J. M., 2007, MNRAS, 381, 263
Bensby T., Feltzing S., Lundström I., Ilyin I., 2005, A&A, 433, 185
Bertone E., Buzzoni A., Chávez M., Rodríguez-Merino L. H., 2008, A&A, 485, 823
Bruzual G., Charlot S., 2003, MNRAS, 344, 1000
Catelan M., Grundahl F., Sweigart A. V., Valcarce A. A. R., Cortés C., 2009, ApJL, 695, L97
Cervantes J. L., Coelho P., Barbuy B., Vazdekis A., 2007, in Vazdekis A., Peletier R. F., eds, IAU Symposium Vol. 241 of IAU Symposium, A new approach to derive [α/Fe] for integrated stellar populations. pp 167–168
Cid Fernandes R., Mateus A., Sodré L., Stasińska G., Gomes J. M., 2005, MNRAS, 358, 363
Coelho P., Bruzual G., Charlot S., Weiss A., Barbuy B., Ferguson J. W., 2007, MNRAS, 382, 498
Feltzing S., Johnson R. A., 2002, A&A, 385, 67
Gallazzi A., Charlot S., Brinchmann J., White S. D. M., 2006, MNRAS, 370, 1106
Koleva M., Prugniel P., Ocvirk P., Le Borgne D., Soubiran C., 2008, MNRAS, 385, 1998
Lawson C. L., Hanson R. J., 1974, Solving least squares problems. Prentice-Hall Series in Automatic Computation, Englewood Cliffs: Prentice-Hall, 1974
Le Borgne D., Rocca-Volmerange B., Prugniel P., Lançon A., Fioc M., Soubiran C., 2004, A&A, 425, 881
Le Borgne J.-F., Bruzual G., Pelló R., Lançon A., Rocca-Volmerange B., Sanahuja B., Schaerer D., Soubiran C., Vílchez-Gómez R., 2003, A&A, 402, 433
MacArthur L. A., Gonzalez J. J., Courteau S., 2009, ArXiv e-prints
Martins L. P., Coelho P., 2007, MNRAS, 381, 1329
Meléndez J., Barbuy B., Bica E., Zoccali M., Ortolani S., Renzini A., Hill V., 2003, A&A, 411, 417
Ocvirk P., Pichon C., Lançon A., Thiébaut E., 2006, MNRAS, 365, 74
Panter B., Jimenez R., Heavens A. F., Charlot S., 2008, MNRAS, 391, 1117
Percival S. M., Salaris M., Cassisi S., Pietrinferni A., 2009, ApJ, 690, 427
Prugniel P., Koleva M., Ocvirk P., Le Borgne D., Soubiran C., 2007, in Vazdekis A., Peletier R. F., eds, IAU Symposium Vol. 241 of IAU Symposium, Analysis of stellar populations with large empirical libraries at high spectral resolution. pp 68–72
Schiavon R. P., Rose J. A., Courteau S., MacArthur L. A., 2005, ApJS, 160, 163
Thomas D., Maraston C., Korn A., 2004, MNRAS, 351, L19
Tojeiro R., Heavens A. F., Jimenez R., Panter B., 2007, MNRAS, 381, 1252
Trager S. C., Faber S. M., Worthey G., González J. J., 2000, AJ, 119, 1645
Vazdekis A., 1999, ApJ, 513, 224
Vazdekis A., Kuntschner H., Davies R. L., Arimoto N., Nakamura O., Peletier R., 2001, ApJL, 551, L127
Vázquez G. A., Leitherer C., 2005, ApJ, 621, 695
Walcher C. J., Böker T., Charlot S., Ho L. C., Rix H.-W., Rossa J., Shields J. C., van der Marel R. P., 2006, ApJ, 649, 692
Walcher C. J., Lamareille F., Vergani D., Arnouts S., Buat V., Charlot S., Tresse L., Le Fèvre O., Bolzonella M., Brinchmann J., Pozzetti L., Zamorani G. e. a., 2008, A&A, 491, 713
Wild V., Kauffmann G., Heckman T., Charlot S., Lemson G., Brinchmann J., Reichard T., Pasquali A., 2007, MNRAS, 381, 543
Wolf M. J., Drory N., Gebhardt K., Hill G. J., 2007, ApJ, 655, 179
Worthey G., Faber S. M., Gonzalez J. J., 1992, ApJ, 398, 69
Zoccali M., Barbuy B., Hill V., Ortolani S., Renzini A., Bica E., Momany Y., Pasquini L., Minniti D., Rich R. M., 2004, A&A, 423, 507